

Global Methane Emissions From Wetlands, Rice Paddies, and Lakes

PAGES 37–38

The current concentration of atmospheric methane is 1774 ± 1.8 parts per billion, and it accounts for 18% of total greenhouse gas radiative forcing [Forster *et al.*, 2007]. Atmospheric methane is 22 times more effective, on a per-unit-mass basis, than carbon dioxide in absorbing long-wave radiation on a 100-year time horizon, and it plays an important role in atmospheric ozone chemistry (e.g., in the presence of nitrous oxides, tropospheric methane oxidation will lead to the formation of ozone). Wetlands are a large source of atmospheric methane, Arctic lakes have recently been recognized as a major source [e.g., Walter *et al.*, 2006], and anthropogenic activities—such as rice agriculture—also make a considerable contribution.

However, the quantification of methane emissions still has large uncertainties. In this article, we identify some causes for the uncertainty; illustrate the challenges of reducing the uncertainty; and highlight opportunities for research from the global perspective and also from the perspective of three principal sources of methane: the Arctic, the Amazon basin, and rice paddies.

Global Perspective

Accurately mapping the global distribution and dynamics of lakes and wetland types is challenging. Currently, estimates of global wetland areas from ground and satellite instruments vary from 1 to 12 million square kilometers. Some existing estimates do not account for small lakes, resulting in underestimates of lake areas by a factor of more than 2 [e.g., Walter *et al.*, 2007]. Further, global characterizations of wetlands and lakes are too coarse to represent significant differences in methane emission rates, and data on seasonal and interannual wetland inundation derived from satellite sensors need to be further developed. Satellite data in combination with ground-level

surveys of vegetation and wetland types should be continued as a means to further develop data on global lake and wetland distribution and extent.

Methane flux measurements, which are lacking from a variety of ecosystems, as noted below, are needed to improve emission estimates and the accuracy of biogeochemical models and atmospheric transport inversion models [e.g., Zhuang and Reeburgh, 2008]. Data acquisition of in situ and satellite atmospheric concentrations and their profiles should be maintained to more

accurately quantify global methane emissions with these models [e.g., Dlugokencky *et al.*, 2003]. Instrumentation for monitoring methane fluxes and concentrations should be a priority.

Controls on, and processes of, biogenic methane emissions are not well understood. We suggest the following research priorities: (1) elucidate the role of permafrost degradation in methane emissions; (2) further examine the effects of the atmospheric deposition of nitrogen and sulfate on methane production and consumption; (3) investigate the microbial community structure and distribution of those microbes responsible for methane production and consumption; and (4) investigate the role of different vegetation types in affecting the exchanges of methane between wetlands and the atmosphere.

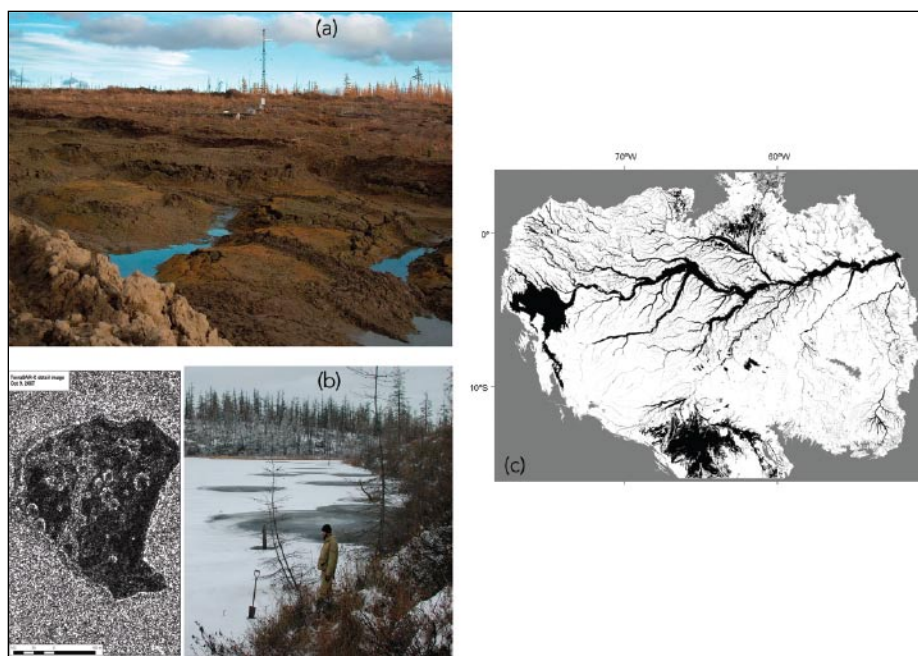


Fig. 1. (a) In the Siberian north, the polygonal net of ice wedges is ubiquitous. In Pleistocene-aged (1.8 million to 10,000 years before present) yedoma (an organic-rich loess with about 2% carbon by mass and with ice content of 50–90% by volume [see Walter *et al.*, 2006]), the tops of ice wedges are usually situated directly beneath the active layer, so the active layer growth will lead to ice wedge melting and the appearance of the polygonal net of deep channels. Ponding of water in these channels causes deep thaw of permafrost, leading to the formation of methane-producing thermokarst lakes. (b) In the Arctic lakes, open holes in early winter lake ice due to seeps of methane bubbling are visible from airplanes and in TerraSAR-X satellite imagery. (c) Floodable area (black) for the Amazon basin below the 500-meter contour, derived from Japanese Earth Resources Satellite 1 (JERS 1) synthetic aperture radar mosaics. Floodable areas are not all inundated simultaneously and may include areas not floodable that are not visible at the scale of the image. These floodable areas are important to methane emissions in the Amazon basin [from Melack and Hess, 2009].

Challenges and Opportunities in the Arctic

The carbon-rich Arctic soils and lakes are underlain with either continuous or discontinuous permafrost, which is a large reservoir of carbon containing 700–950 petagrams of carbon in its top 1–25 meters (Figure 1a) [Zimov *et al.*, 2006]. Currently, methane is released from both thaw lakes and soils (Figure 1b) [Walter *et al.*, 2006]. An increase in permafrost degradation and the shoreline erosion of existing lakes along with the formation of new permafrost-thawing lakes is expected, and these changes could increase methane emissions from these lakes by several orders of magnitude [Walter *et al.*, 2007].

As permafrost thawing develops, increased linear erosion associated with thaw lake expansion and migration could lead to stream channel erosion and lake drainage. For instance, in the discontinuous permafrost zone of West Siberia, this process has already begun to lead to a decrease in lake area. In West Siberia's far north, deep, cold ice wedges comprise more than 80% of permafrost volume and are often covered with only 0.5 meters of soil. Minor increases in summer soil active layer thickness will initiate the thaw of ice wedges in permafrost. Once the melting process begins, the disappearance of these large ice bodies will result in dramatic changes in land surface driven by active thaw erosion, thawing tens of meters into permafrost.

In upland environments, permafrost-thawing ponds will form in the channels that appear above thawing ice wedges. The bottoms of these ponds remain unfrozen throughout winter, actively producing and emitting methane year round. On wet lowlands, the development of a polygonal system of channels can increase the drainage regime and partially dry the landscape, increasing areas for methane oxidation in dry surface soils and reducing the net methane emissions from this environment [e.g., Smith *et al.*, 2005]. Thus, modeling landscape relief and drainage patterns should be a priority in predicting the response of Arctic lake and wetland methane to permafrost thaw.

The key questions in estimating methane emissions from permafrost environments are as follows: (1) What is the size of the permafrost carbon pool? (2) Which fraction of this pool will be converted to methane upon thaw? (3) Which fraction of the permafrost carbon pool will thaw under anaerobic versus aerobic conditions? (4) What is the role of methane oxidation in controlling methane emissions?

Challenges and Opportunities in the Amazon Basin

Tropical wetlands are a major source of atmospheric methane. However, regional estimates of emissions from these wetlands

have large uncertainties, and many tropical systems lack measurements of emissions. For the Amazon basin, Melack *et al.* [2004] combined passive and active microwave remote sensing of the temporally varying extent of inundation and vegetation with field measurements to estimate that methane emissions are 22 teragrams per year. Further improvements in these estimates will require field campaigns in undersampled environments including extensive savannas, high-elevation wetlands, narrow riparian zones along streams, and small rivers.

Another important area in northern South America is the upper Negro River basin, because it includes an approximately 80,000-square-kilometer area with seasonally flooded emergent grasses and sedges, areas with shrubs or palms, and flooded forests—all of which are methanogenic habitats. Year-round measurements of diffusive and bubble emissions of methane in these organic-rich environments, and the influences of habitat, water depth, variation in hydrostatic pressure, dissolved oxygen, and temperature, have recently been determined by Belger [2007]. Similar measurements are needed in the Pantanal in central South America, the Llanos de Moxos, largely in eastern Bolivia, the Roraima savannas of northern Brazil, and the swamps of lowland Peru, although many of the wetlands in these areas are situated in interfluvial regions, making access very difficult.

Methane emissions from Amazonian reservoirs also have been measured occasionally at the Samuel, Tucuruí, and Curuá-Una reservoirs (located in the central and eastern Amazon basin in Brazil), and more extensively in the Balbina reservoir (located north of Manaus in the central Amazon), and the potential importance of downstream degassing in tropical reservoirs has been demonstrated [Kemenes *et al.*, 2007]. Further measurements with improved methodology are needed to evaluate the extent of degassing.

The entire lowland Amazon basin—which, because of its large area of methanogenic habitats, is important for methane emissions—has an estimated floodable area of 0.8 million square kilometers (Figure 1c). The improved topography provided by the Shuttle Radar Topography Mission's interferometric synthetic aperture radar data, in combination with runoff models, should improve the estimation of the extent of the methane-producing habitats.

Measuring and modeling inundation and vegetation dynamics in seasonally flooded savannas, palm swamps, riparian zones, and wetlands in mountainous terrain are top research priorities, and flux measurements in the Amazon should continue.

Challenges and Opportunities in Rice Paddy Emission Studies

Seasonally averaged methane flux (SAF) from rice paddies ranges from 2 to

40 milligrams of methane per hour per square meter. In part, this range reflects the different ecosystems under which rice is grown (e.g., irrigated, rain-fed, deepwater, and so forth), and water management (e.g., continuous versus intermittently flooded), as longer inundation periods produce higher fluxes. It also reflects differences in input organic matter, soil type, and crop phenology, among other variables. In addition, SAFs from the same field in side-by-side plots are observed to vary over the emission season by a factor of 2 to 4, evidently owing to field inhomogeneities. Sampling of methane flux in paddies using the standard method of three replicates can produce SAFs that vary by 40–60% [Khalil and Butenhoff, 2008].

Paddy emissions are sensitive to farming practices that can change in response to economic and political pressures [Khalil and Rasmussen, 1993]. In China, conservation has reduced the amount of water used for paddy irrigation, while bans on biomass burning have returned otherwise burnt crop residue to the field. Manure use has declined in favor of inorganic fertilizers. Quantifying these changes is vital for determining accurate inventories, but it remains challenging. Many farming practices are not officially recorded and are available only through personal communication. Interviews with farmers have yielded important information, but more extensive surveying is required.

Extrapolating paddy fluxes to larger scales requires geospatial data on rice production and controlling factors. Current agricultural census data are insufficient to meet increasing resolution demands (<10 kilometers). Process-based modeling and remote sensing are being used to fill some of these gaps. For example, satellite-derived vegetation indices can locate paddies on the basis of crop phenology. These techniques can map not only spatial coverage, but also temporal changes.

Only in recent years have scientists been able to use remote sensing to detect methane emissions. Placing precise constraints on individual sources of methane emissions is difficult because all sources contribute to the signal, but satellite-derived measurements have put upper level constraints on rice emissions (e.g., <80 teragrams of methane per year [Frankenberg *et al.*, 2005; see also Xiong *et al.*, 2008]). Further refinements to the paddy emission budget will benefit from a longer time series of satellite data and from regional ground-based networks closer to paddy emissions. These efforts will be vital to verifying and monitoring national commitments to greenhouse gas emission treaties.

In conclusion, to accurately quantify global methane emissions, the priorities are improving biogeochemical and atmospheric inversion and transport modeling approaches and developing high-resolution data on wetlands and lake distribution and their changes using remote sensing data validated with ground surveys. In addition, the acquisition of in situ and satellite data

of methane fluxes and concentrations plus ancillary environmental data is needed for many areas.

Acknowledgments

This article is a contribution of the Methane Working Group of the National Center for Ecological Analysis and Synthesis, University of California, Santa Barbara. The research is also supported by U.S. National Science Foundation grants ARC-0554811 and EAR-0630319 to Q. Zhuang and by NASA's Large-Scale Biosphere-Atmosphere Experiment in Amazonia program.

References

Belger, L. (2007), Fatores que influem na emissão de CO₂ e CH₄ em áreas alagáveis interfluviais do médio Rio Negro, Ph.D. thesis, Univ. Fed. da Amazonas and Inst. Nac. de Pesquisas da Amazônia, São Paulo, Brazil.

Dlugokencky, E. J., et al. (2003), Atmospheric methane levels off: Temporary pause or a new steady state?, *Geophys. Res. Lett.*, 30(19), 1992, doi:10.1029/2003GL018126.

Forster, P., et al. (2007), Changes in atmospheric constituents and in radiative forcing, in *Climate Change 2007: The Physical Science Basis—Contribution of Working Group I to the Fourth Assess-*

ment Report of the Intergovernmental Panel on Climate Change, edited by S. Solomon et al., pp. 131–234, Cambridge Univ. Press, Cambridge, U.K.

Frankenberg, C., et al. (2005), Assessing methane emissions from global space-borne observations, *Science*, 308, 1010–1014.

Kemenes, A., B. R. Forsberg, and J. M. Melack (2007), Methane release below a hydroelectric dam, *Geophys. Res. Lett.*, 34, L12809, doi:10.1029/2007GL029479.

Khalil, M. A. K., and C. L. Butenhoff (2008), Spatial variability of methane emissions from rice fields and implications for experimental design, *J. Geophys. Res.*, 113, G00A09, doi:10.1029/2007JG000517.

Khalil, M. A. K., and R. A. Rasmusussen (1993), Decreasing trend of methane: Unpredictability of future concentrations, *Chemosphere*, 26, 803–814.

Melack, J. M., and L. L. Hess (2009), Remote sensing of the distribution and extent of wetlands in the Amazon basin, in *Amazonian Floodplain Forests: Ecophysiology, Ecology, Biodiversity and Sustainable Management*, *Ecol. Stud. Ser.*, edited by W. J. Junk and M. Piedade, Springer, New York, in press.

Melack, J. M., et al. (2004), Regionalization of methane emissions in the Amazon Basin with microwave remote sensing, *Global Change Biol.*, 10, 530–544.

Smith, L. C., Y. Sheng, G. M. MacDonald, and L. D. Hinzman (2005), Disappearing Arctic lakes, *Science*, 308, 1429, doi:10.1126/science.1108142.

Walter, K. M., et al. (2006), Methane bubbling from Siberian thaw lakes as a positive feedback to climate warming, *Nature*, 443, 71–75, doi:10.1038/nature05040.

Walter, K. M., et al. (2007), Methane bubbling from northern lakes: Present and future contributions to the global methane budget, *Philos. Trans. R. Soc.*, 365(1856), 1657–1676.

Xiong, X., et al. (2008), Methane plume over South Asia during the monsoon season: Satellite observation and model simulation, *Atmos. Chem. Phys. Discuss.*, 8, 13,453–13,478.

Zhuang, Q., and W. S. Reebergh (2008), Introduction to special section on Synthesis of Recent Terrestrial Methane Emission Studies, *J. Geophys. Res.*, 113, G00A02, doi:10.1029/2008JG000749.

Zimov, S. A., E. A. Schuur, and F. S. Chapin (2006), Climate change: Permafrost and the global carbon budget, *Science*, 312, 1612–1613, doi:10.1126/science.1128908.

Author Information

Qianlai Zhuang, Departments of Earth and Atmospheric Sciences and Agronomy, Purdue University, West Lafayette, Indiana; E-mail: qzhuang@purdue.edu; John M. Melack, University of California, Santa Barbara; Sergey Zimov, North-East Science Station, Cherskii, Sakha Republic (Yakutia), Russia; Katey M. Walter, University of Alaska Fairbanks; and Christopher L. Butenhoff and M. Aslam K. Khalil, Portland State University, Portland, Oreg.

Monitoring Algal Blooms in a Southwestern U.S. Reservoir System

PAGES 38–39

In recent years, several studies have explored the potential of higher-resolution sensor data for monitoring phytoplankton primary production in coastal areas and lakes. Landsat data have been used to monitor algal blooms [Chang et al., 2004; Vincent et al., 2004], and Moderate Resolution Imaging Spectroradiometer (MODIS) 250-meter and Medium Resolution Imaging Spectrometer (MERIS) full-resolution (300-meter) bands have been utilized to detect cyanobacterial blooms [Reinart and Kutser, 2006] as well as to monitor water quality [Koponen et al., 2004].

Field sampling efforts and MODIS 250-meter data are now being combined to develop a cost-effective method for monitoring water quality in a southwestern U.S. reservoir system. In the Phoenix, Ariz., metropolitan area, the Salt River reservoirs supply more than 3.5 million people, a population expected to rise to more than 6 million by 2030. Given that reservoir capacities have physical limitations, maintaining water quality will become critical as the population expands. Potentially noxious algal blooms that can release toxins and may affect water quality by modifying taste and odor have become a major concern in recent years. While frequent field sampling regimes are expensive, satellite imagery can be applied cost-effectively to monitor algal biomass trends remotely, and this information could provide early warning of blooms in these reservoirs.

Current Study

The Salt River reservoir system comprises four reservoirs that are managed for a combination of water provision and hydroelectric power generation, as well as for recreational activities. This study focused on the two end-member reservoirs, Roosevelt Lake and Saguaro Lake, on the basis that they are the inflow and outflow ecological communities within the system and may be considered as representative of the plankton ecology of the reservoir system overall. Also, both reservoirs are large enough to produce a reasonable sample size of uncontaminated 250-meter pixels. Roosevelt Lake (111.1°W, 33.7°N) is the top reservoir, with a surface area of 9698 hectares. When full, the reservoir is 36 kilometers long and 76 meters deep. In contrast, Saguaro Lake (111.5°W, 33.6°N), the lowest reservoir, at 465-meter elevation, is much smaller, with a reservoir basin of 2.5 kilometers × 1.0 kilometer.

Monthly field sampling began in February 2007 and was conducted on one transect on each reservoir. At regular points along each transect, measurements of temperature and transparency were taken and water samples were collected for chlorophyll *a* and microscopic analysis.

Satellite Analysis

The daily MODIS Aqua 250-meter level 2 georectified (L2G) surface reflectance

products were obtained for each field collection date from the Land Processes Distributed Active Archive Center (LP DAAC; <http://edcdaac.usgs.gov/main.asp>). These surface reflectance images are produced from two bands (645 and 856 nanometers), each of which has 250-meter spatial resolution. Each file is georectified (i.e., pixels are assigned geographic coordinates) and adjusted for aerosols, atmospheric gases, and high, thin clouds.

The regression analyses of the in situ data and the equivalent satellite reflectance values produced different results for each lake. In both Roosevelt Lake and Saguaro Lake, a fourth-order polynomial provided the best fit ($r^2_{\text{Roosevelt}} = 0.871$ and $r^2_{\text{Saguaro}} = 0.694$) to the data. The observed differences in performance between these regression equations were large enough to warrant the use of lake-specific algorithms for the subsequent time series analysis.

Satellite-Derived Chlorophyll *a* Time Series

The time series of chlorophyll *a* estimates for 2007 (363 available images) for Roosevelt Lake produced 221 valid estimates with predicted chlorophyll *a* values ranging from 0.32 to 7.13 milligrams per cubic meter and a mean of 3.51 milligrams per cubic meter (Figure 1a). The remaining 142 estimates (39% of the 363 available images) were excluded as part of a rudimentary quality check because either high cloud cover obscured the area, excessive cloud cover skewed the atmospheric correction performed during data processing, or the image data were corrupted resulting in poor-quality pixels.